

Article

Application of Oxovanadium Complex Stabilized by *N,N,N,N*-Chelating Ligand in Air-Drying Paints

Iva Charamzová¹, Jaromír Vinklárěk², Petr Kalenda¹ and Jan Honzík^{1,*}

¹ Institute of Chemistry and Technology of Macromolecular Materials, Faculty of Chemical Technology, University of Pardubice, Studentská 573, 532 10 Pardubice, Czech Republic; st34516@student.upce.cz (I.C.); petr.kalenda@upce.cz (P.K.)

² Department of General and Inorganic Chemistry, Faculty of Chemical Technology, University of Pardubice, Studentská 573, 532 10 Pardubice, Czech Republic; jaromir.vinklarek@upce.cz

* Correspondence: jan.honzicek@upce.cz; Tel.: +420-46603-7229

Received: 23 April 2018; Accepted: 25 May 2018; Published: 28 May 2018



Abstract: New vanadium-based drier, stabilized with macrocyclic chelating ligand, is described. Its drying activity was established on solvent-borne alkyd resins of different oil-length modified by soybean oil. The test coatings were characterized by standardized mechanical tests as well as spectroscopic methods. Time-resolved infrared spectroscopy was used for determination of kinetic parameters of the autoxidation process while the EPR (electron paramagnetic resonance) spectroscopy enabled confirmation of stability of oxovanadium(IV) species in the cured films. The obtained experimental data revealed promising catalytic activity of the oxovanadium(IV) compound stabilized with *N,N,N,N*-chelating ligand at low concentration. At 0.03 wt % of metal in dry matter content, it shows short total dry times not exceeding 12 h while commercial cobalt(II) 2-ethylhexanoate is, at the same concentration, considerably lower active with total dry times 15.4 h (alkyd of short oil-length) and >24 h (alkyd of medium oil-length).

Keywords: oxovanadium; air-drying paint; alkyd resin; autoxidation

1. Introduction

Alkyds became a preeminent binder for coatings since the 1950s and they are still one of the most widespread in the paint production industry [1]. As chemicals, solvent-borne alkyds are synthetic polyesters usually produced from glycerol, vegetable oils (triglycerides of polyunsaturated fatty acids) and phthalic anhydride [2,3]. Curing of alkyd resins is based on oxo-polymerization of fatty acids chains containing sensitive C–H bonds on bis-allylic moiety [4]. This process, also known as autoxidation, includes a series of radical reactions within termination step 3-dimensional crosslinked film (Figure 1) [5]. Due to its complexity, the autoxidation was studied on various model systems (e.g., ethyl linoleate, (*Z,Z*)- and (*E,E*)-nona-3,6-diene, *tert*-butyl hydroperoxide) in order to get insight into mechanism of the crosslinking processes [6–8].

At ambient temperature, the autoxidation is very slow, and therefore the use of catalysts, so-called driers, is necessary in common alkyd-based paint systems. They are divided into three groups: primary, secondary and tertiary driers [2,9]. Primary driers are redox-active transition metal compounds accelerating the autoxidation process of air-drying paints. Their ability to change oxidation state can enforce the alkyl radical formation through hydrogen abstraction [10]. Nevertheless, their main function is to accelerate hydroperoxide decomposition (Figure 1). They can also catalyze other reactions involved in the crosslinking process (e.g., ene-reaction, 1,2- and 1,4-addition) [11]. The primary driers usually form the crosslinked polymeric films fast but not homogeneously. Due to limited air-oxygen diffusion, the coatings are cured from top surface down to the substrate which is why they are often

called “surface driers”. Cobalt(II) carboxylates are widely used in the paint production industry mainly due to their strong drying activity and low price [9].

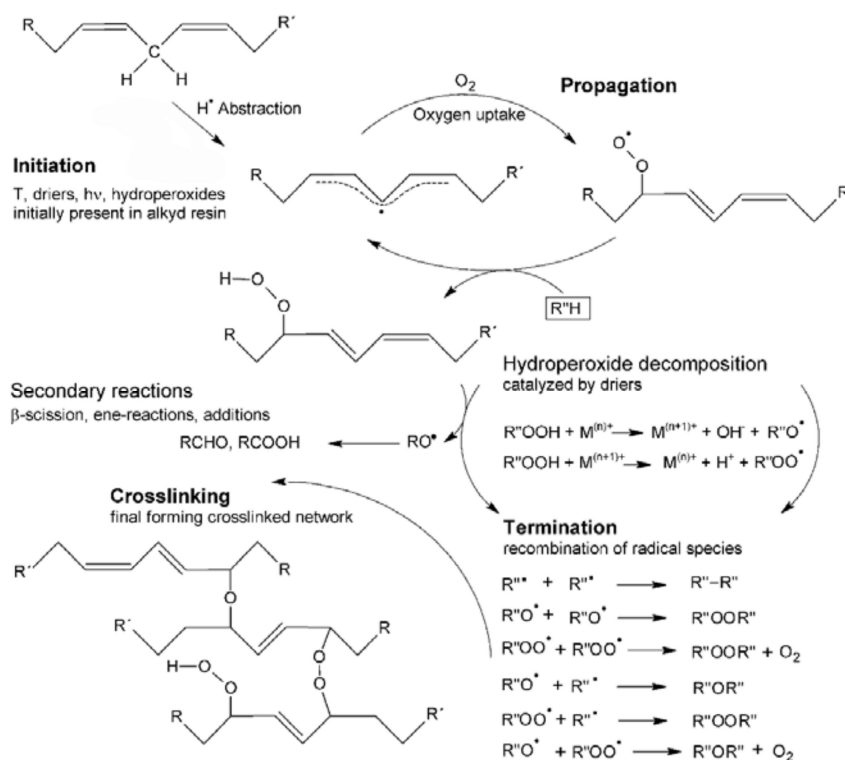


Figure 1. Simplified mechanism of autoxidation process accelerated by primary driers.

Secondary driers do not accelerate autoxidation process themselves but only in conjunction with primary driers. They perform as Lewis acidic co-catalysts, whose help to control homogeneity of crosslinking process as a function of depth led to their alternative name “through driers”. Commercial secondary driers include carboxylates of zirconium, bismuth and aluminum. Tertiary driers (also known as auxiliary) help to regulate oxygen uptake and prevent inactivation of primary driers. They include calcium, zinc, lithium and potassium carboxylates [2,12].

Acknowledged studies have revealed that cobalt(II) compounds, widely used in the paint production industry as primary driers, are genotoxic and carcinogenic, which may in near future lead to legislative restrictions of their use [13–15]. This situation stimulates a search for non-toxic cobalt-free primary driers applicable in industry. Although several manganese [16–18] and iron complexes [7,9,19–22] show promising drying activity, most of them still suffer from some disadvantages such as low activity at ambient temperature, intense coloration or low solubility in paint formulations. Our investigation, in this field, has been focused on vanadium-based alternatives due to their low overall toxicity [23,24]. Recently, we have demonstrated strong drying activity for oxovanadium(IV) diketonates [25,26] and oxovanadium(IV) 2-ethylhexanoate [27] at considerably lower concentrations than are applicable for commercial cobalt-based driers.

The present study is aimed at stabilization of oxovanadium(IV) species by chelating effect. Drying activity of the complex bearing macrocyclic *N,N,N,N*-chelating ligand (VO; Figure 2a) will be established in commercial solvent-borne alkyd resins and compared with commercial cobalt-base drier (Co; Figure 2b). The effects of the primary driers on kinetics of the autoxidation process will be followed by spectroscopic methods.

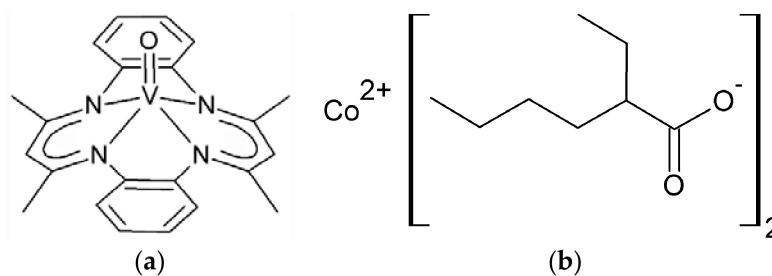


Figure 2. Primary driers under the study: (a) VO; (b) Co.

2. Materials and Methods

2.1. Chemicals

Oxovanadium compound VO was prepared according to literature procedure [28]. It was grinded in a mortar to desired particle size immediately before use. Alkyd resins modified by soybean oil CHS-ALKYD S 401 X 55 (S401; short oil-length, AV (acid value) = 7 mg KOH/g) and CHS-ALKYD S 471 X 60 (S471; medium oil-length, AV = 6 mg KOH/g) were supplied by Spolchemie (Ústí nad Labem, Czech Republic). Cobalt(II) 2-ethylhexanoate solution (Co; 65 wt % in mineral spirits; Sigma-Aldrich, St. Louis, MO, USA) was used as obtained without further modifications.

2.2. Film Preparation

The calculated amount of the drier was weighted on analytical balance, treated with alkyd resin (5 g), dispersed for 5 min and sonicated by ultrasound for 3 min to give clear formulation. The test films were prepared by frame applicators with different slots (76 μm for measurements of drying time, 150 μm for film hardness measurements and 100 μm for kinetic experiments). All drier concentrations are reported as metal concentrations and given in wt % based on dry matter content of given alkyd resin.

2.3. Film Drying Time

Measurements of drying time were performed on a Beck Koller Drying Time Recorder (BYK-Gardner, Geretsried, Germany) according to ASTM D5895-03 [29] and under standard laboratory conditions ($T = 23\text{ }^{\circ}\text{C}$, rel. humidity = 50%). Films on glass test strips (305 mm \times 25 mm \times 2 mm) were placed into holders of the device. Holder with hemispherical-ended needle ($D = 1\text{ mm}$) was placed to beginning of wet film clamped in horizontal direction with 5 g weight. The straight-line groove resulting during 24 h is usually used for determination of set-to-touch time (τ_1), tack-free time (τ_2), dry-hard time (τ_3) and dry-through time (τ_4) [29]. In our case, the casted films are set-to-touch dry ($\tau_1 = 0$) and only tack-free time (τ_2) and total time of film curing (dry-hard time, τ_3) were observed due to specific properties of given binders. During the first stage of film drying ($t = 0 \sim \tau_2$), the solvents are evaporated and sol-gel transition proceeds. The needle gives bold and uninterrupted line. During the second stage ($t = \tau_2 \sim \tau_3$) the needle starts to climb over the film. It tears formed layer and lefts ragged groove. After τ_3 , no visible mark is observed on the film ($\tau_3 \equiv \tau_4$).

2.4. Determination of Film Hardness

Film hardness development was monitored using a Persoz Type Pendulum Hardness Tester (Elcometer, Manchester, UK). The method is based on registering the number of pendulum swings. The amplitude of oscillation of a pendulum placed on examined film decreases more rapidly the softer the surface is. All measurements were carried out in conformity with ISO 1522 [30] and under standard laboratory conditions ($T = 23\text{ }^{\circ}\text{C}$, rel. humidity = 50%). Films were prepared on glass plates (100 mm \times 200 mm \times 4 mm) and their properties were measured within 100 days. The measured

values were related to the hardness of a glass standard and expressed as relative hardness. The error in determination of surface hardness was estimated to be 0.5%.

2.5. FTIR Spectroscopy

All infrared spectra were collected on FTIR (Fourier transform infrared spectroscopy) spectrometer Nicolet iS50 (Thermo Fisher Scientific, Waltham, MA, USA; No. of scans: 32, data spacing: 0.5 cm^{-1}) in the range of $4000\text{--}500\text{ cm}^{-1}$. Characterization of VO was done on a built-in all-reflective diamond ATR (attenuated total reflectance) while time-resolved spectra of alkyd coatings were measured in the standard transmission mode. The samples of alkyd formulations, used for kinetic studies, were applied on NaCl crystal using film applicator with $100\text{ }\mu\text{m}$ slot and placed into the climate chamber ($T = 23 \pm 1\text{ }^\circ\text{C}$, rel. humidity = $50\% \pm 2\%$). The spectra were registered every 5 min. Collected series of the spectra were integrated using fixed two-point baseline in the bounds $3014\text{--}2997\text{ cm}^{-1}$ [$\nu_s(\text{cis-CH=CH})$, isolated double bond] and $1011\text{--}947\text{ cm}^{-1}$ (*cis-trans* conjugated C=C-H wagging). Rate coefficient ($k_{\text{CH,max}}$) was obtained from logarithmic plot of integrated area of $\nu_s(\text{cis-CH=CH})$ as the steepest slope.

2.6. EPR Spectroscopy

EPR (electron paramagnetic resonance) spectra were measured on Miniscope MS 300 spectrometer (Magnettech, Berlin, Germany) in microwave X-band (9.5 GHz). The apparatus was gauged on DPPH value ($g_{\text{iso}} = 2.0036 \pm 2$). Solution spectrum was measured in dichloromethane in glass capillary (ID = 0.5 mm) at room temperature (293 K). Frozen solution spectrum was measured in mixture dichloromethane/ethanol (1:1) in quartz tube (ID = 3 mm) at 123 K. Solid spectra of cured film were measured in quartz tubes (ID = 5 mm) at 293 K. The films were scratched off after 100 days of curing from glass plates ($100\text{ mm} \times 200\text{ mm} \times 4\text{ mm}$).

3. Results and Discussions

3.1. Synthesis and Characterization

Oxovanadium complex VO (Figure 2) was prepared from commercially available $\text{VO}(\text{acac})_2$ and freshly prepared *N,N,N,N*-chelating ligand [31] by exchange reaction according to literature procedure [28]. The prepared complex was characterized by spectroscopic methods. The infrared spectrum shows a strong band of V=O stretching at 971 cm^{-1} , which correlates well with recently published data using the same sampling method [32]. Paramagnetic nature of the title compound enables the use of EPR spectroscopy for characterization. Isotropic spectrum, obtained in dichloromethane solution at ambient temperature, shows strong hyperfine coupling (Figure 3a) typical for interaction of unpaired electron with one nucleus of ^{51}V ($I = 7/2$), whose natural abundance is 99.8% [33]. The observed isotropic hyperfine coupling constant ($A_{\text{iso}} = 88.7 \times 10^{-4}\text{ T}$) as well as the isotropic *g*-factor ($g_{\text{iso}} = 1.978$) near the values reported in literature [34]. The absence of another EPR active species in the spectrum proves full conversion of the exchange reaction. Due to strong sensitivity of the EPR parameters on changes in coordination sphere of the central metal, contamination with starting $\text{VO}(\text{acac})_2$ ($A_{\text{iso}} = 108.7 \times 10^{-4}\text{ T}$, $g_{\text{iso}} = 1.969$) [25] or oxovanadium(IV) side products should be easily recognizable. Anisotropic spectrum of the title compound was obtained for frozen solution in a 1:1 mixture of dichloromethane and ethanol (Figure 3b). The spectrum is axial symmetric ($A_{\parallel} = 165.0 \times 10^{-4}\text{ T}$, $A_{\perp} = 52.5 \times 10^{-4}\text{ T}$, $g_{\parallel} = 1.959$, $g_{\perp} = 1.969$), which corresponds well with its square-pyramidal structure.

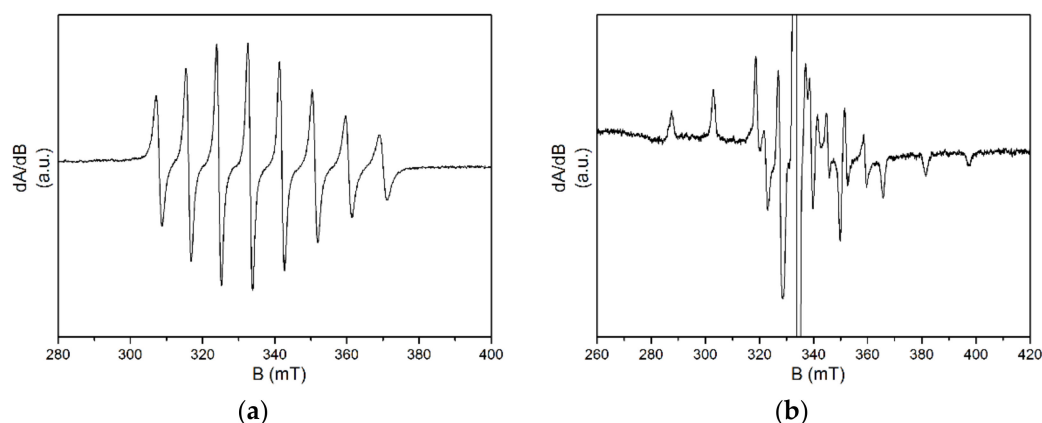


Figure 3. EPR spectra of VO (a) in CH_2Cl_2 solution and (b) in frozen 1:1 mixture of CH_2Cl_2 /ethanol.

3.2. Drying Activity

Commercial solvent-borne alkyd resins of short (S401) and medium oil-length (S471) were used for evaluation of drying activity of the complex VO. The measurements on test coatings were performed at concentration range 0.1–0.005 wt % of the drier in the dry matter content of given alkyd resin and compared with performance of commercial cobalt-based drier Co. The tack-free time (τ_2), total drying time (τ_3) and relative hardness ($H_{\text{rel},10}$, $H_{\text{rel},100}$) are summarized in Table 1.

In the alkyd resins of short and medium oil-length, the title vanadium compound (VO) shows satisfactory drying activity up to concentration 0.03 wt % as evidenced from short total drying times not exceeding 12 h (Table 1). The tack-free times (τ_2) as well as total drying times (τ_3) are, at given concentration, considerably shorter than observed for commercial drier Co. The only exception is long total drying time of the formulation VO/S471 at 0.1 wt %, which was attributed to overdose effect. The main advantage of the vanadium-based drier is a very fast sol-gel transition even at low concentration as evidenced from low values of τ_2 . Indeed, the formulations of S401 and S471 at metal concentration 0.005 wt % give the tack-free films already within 2.7 and 13.8 h, respectively. Alkyd resins treated with VO give films of final hardness comparable to formulations of cobalt-based drier. The values obtained after 100 days of curing ($H_{\text{rel},100}$) are suitable for common economic primers and anticorrosive coatings.

We note that VO does not reach as short total dry times as highly-soluble oxovanadium(IV) 2-ethylhexanoate [27] or acetylacetonates decorated with long alkyl tails [26]. The main advantage of VO is higher stability at ambient conditions that is beneficial for long-term storage. Indeed, the later compounds are sensitive to air-oxygen and have to be stored under inert atmosphere.

Table 1. Drying times and relative hardness of alkyd films dried with VO and Co.

Conc. (wt %)	Drier/Alkyd	τ_2^a (h)	τ_3^b (h)	$H_{\text{rel},10}^c$ (%)	$H_{\text{rel},100}^d$ (%)	Drier/Alkyd	τ_2^a (h)	τ_3^b (h)	$H_{\text{rel},10}^c$ (%)	$H_{\text{rel},100}^d$ (%)
0.1	VO/S401	0.6	6.2	32.1	58.0	VO/S471	4.5	8.1	23.9	53.1
0.06		1.5	6.5	22.2	50.8		5.7	9.3	19.5	53.7
0.03		1.5	10.8	29.8	55.4		5.8	10.6	21.1	52.4
0.01		2.3	12.3	32.1	54.0		7.7	17.7	20.5	51.4
0.005		2.7	16.9	34.1	53.7		13.8	>24	35.7	50.6
0.1	Co/S401	5.5	7.6	25.9	61.2	Co/S471	5.2	6.7	20.7	54.1
0.06		2.7	6.9	35.3	58.5		7.7	9.5	20.6	53.7
0.03		5.5	15.4	35.8	57.4		19.2	>24	22.4	49.8
0	S401	>24	>24	6.8	41.9	S471	>24	>24	2.4	33.8

^a: Tack-free time; ^b: Total drying time; ^c: Relative hardness after 10 days of curing; ^d: Relative hardness after 100 days of curing.

3.3. Time-Resolved FTIR Spectroscopy

The kinetics of autoxidation process, responsible for the curing of the alkyd resins, was investigated by time-resolved infrared spectroscopy. This method enables the following of the propagation step of the autoxidation process (Figure 1) through development of C–H stretching band at 3008 cm^{-1} , which was assigned to the moiety with isolated *cis*-double bonds [$\nu_a(\text{cis-C=C-H})$] [22]. Decreasing of the band intensity is shown in Figure 4 for alkyd formulations of S401 and S471 treated with 0.03 wt % of appropriate drier.

All four formulations under the kinetic study show more than 50% conversion upon 24 h of curing as evident from development of the integral plot in linear scale (Figure 4a). Their kinetic behavior is typical for a reaction of pseudo-first order up to ~50% conversion that approximately corresponds to the period when coatings stay saturated with air-oxygen. It is apparent from a linear part of the logarithmic plots shown in Figure 4b. The vanadium-based drier VO exhibits very different kinetic parameters from Co (Table 2). In alkyd resin of short oil-length (S401), VO shows much smaller rate coefficient ($-k_{\text{CH,max}}$) and its better drying performance is due to the absence of induction time (IT).

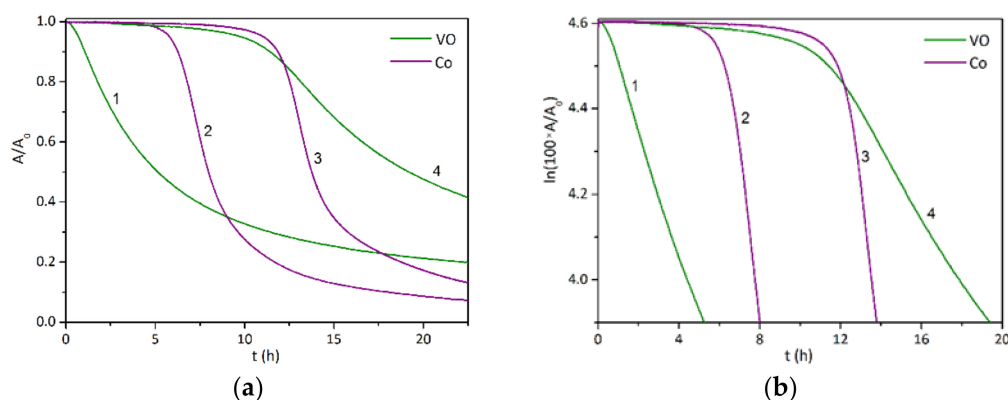


Figure 4. Time-dependent integral plots of the [$\nu_a(\text{cis-C=C-H})$] in alkyd films: (a) In linear scale; (b) In logarithmic scale. Following formulations were studied: (1) 0.03 wt % VO/S401; (2) 0.03 wt % Co/S401; (3) 0.03 wt % Co/S471; (4) 0.03 wt % VO/S471.

The autoxidation process of alkyd resin S471 is slower due to lower polarity caused by higher content of non-polar fatty acid chains. Indeed, the formulations VO/S471 and Co/S471 show considerably longer induction times than VO/S401 and Co/S401, respectively. Nevertheless, the rate coefficients are near the values obtained for appropriate alkyd formulations of short-oil length. Table 2 further summarizes values of t_{conj} , which is estimated as a maximum on the time-dependent integral plot of the band at 989 cm^{-1} assigned to *cis-trans* conjugated C=C–H wagging. This point can be considered as the end of extensive alkyd oxidation and the addition of the radicals on the conjugated double bond system predominates.

Table 2. Kinetic data of the autoxidation process at metal concentration 0.03 wt %.

Formulation	IT (h)	$-k_{\text{CH,max}}$ (h^{-1})	t_{conj} (h)
VO/S401	–	0.17	9.1
Co/S401	6.2	0.43	10.5
VO/S471	10.5	0.09	26.6
Co/S471	12.0	0.43	15.8

3.4. EPR Spectra of Cured Films

EPR spectra of the alkyd coatings treated with VO were measured after 100 days of curing at ambient temperature (Figure 5). Formulations of both alkyd resins give the anisotropic spectra with

well-resolved hyperfine structure of axial symmetry ($A_{\parallel} = 193.2 \times 10^{-4}$ T, $A_{\perp} = 73.6 \times 10^{-4}$ T, $g_{\parallel} = 1.934$, $g_{\perp} = 1.980$). The observed species has considerably stronger hyperfine coupling (A_{\parallel} and A_{\perp}) than observed in the inert solvents. This observation reveals that VO works as a stable precatalyst generating, after dissolution in the alkyd resin, the catalytically active species, whose composition was not fully elucidated. Nevertheless, the EPR data imply C_{4v} -symmetrical coordination sphere of vanadium(IV) with strong ionic character of the bonds V–X. Such demands is fulfilled by square-pyramidal oxovanadium(IV) species, which basal plane is occupied by oxygen donor atoms of the non-esterified carboxylate groups or polyester backbone. We note that virtually the same active species was previously observed in cured alkyd coatings of less stable oxovanadium(IV) precatalysts [26,27].

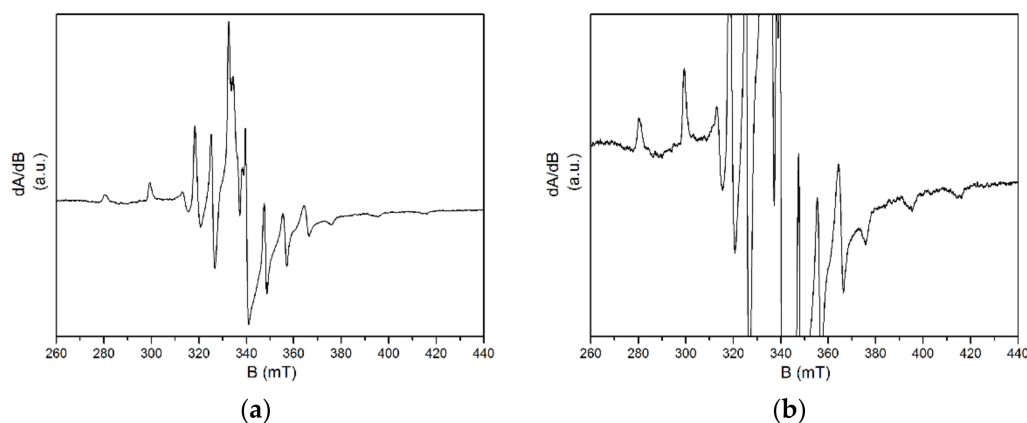


Figure 5. EPR spectrum of the coating VO/S401 cured for 100 days: (a) Full spectrum; (b) Magnification of weak peaks.

4. Conclusions

This study has demonstrated a promising drying activity of VO in two solvent-borne alkyd resins modified with soybean oil. This drier shows optimal performance at considerably lower metal concentration than observed in the case of a commercial drier Co. Indeed, standard mechanical tests revealed that the performance of VO at metal concentration 0.03 wt % is comparable with Co at concentration recommended by supplier (0.06–0.1 wt %). Kinetic study, performed on formulations treated with VO, has shown a relatively low rate coefficient of the autoxidation process suggesting that its very good drying activity is probably caused by fast sol-gel transition. The EPR spectroscopic measurements, performed on cured alkyd coatings, proved that oxovanadium(IV) species, generated after dissolution of VO in formulation, is not consumed upon autoxidation process and works as a true catalyst.

Author Contributions: Conceptualization, I.C., J.V., P.K. and J.H.; Investigation, I.C., J.V. and J.H.; Writing-Original Draft Preparation, I.C.; Writing-Review & Editing, J.H.; Supervision, J.V. and P.K.

Funding: This research was funded by Ministry of Education, Youth and Sports of the Czech Republic (No. UPA SG380006).

Conflicts of Interest: The authors declare no conflict of interest.

References

1. Jones, F.N. Alkyd resins. In *Ullmann's Encyclopedia of Industrial Chemistry*; Wiley-VCH Verlag GmbH & Co. KGaA: Weinheim, Germany, 2012; pp. 429–444. [[CrossRef](#)]
2. Soucek, M.D.; Khattab, T.; Wu, J. Review of autoxidation and driers. *Prog. Org. Coat.* **2012**, *73*, 435–454. [[CrossRef](#)]
3. Hofland, A. Alkyd resins: From down and out to alive and kicking. *Prog. Org. Coat.* **2012**, *73*, 274–282. [[CrossRef](#)]
4. Deffar, D.; Soucek, M.D. Synergistic effect of driers on soybean oil-based ceramer coatings. *J. Coat. Technol.* **2001**, *73*, 95–104. [[CrossRef](#)]

5. Van Gorkum, R.; Bouwman, E. The oxidative drying of alkyd paint catalysed by metal complexes. *Coord. Chem. Rev.* **2005**, *249*, 1709–1728. [[CrossRef](#)]
6. Hubert, J.C.; Venderbosch, R.A.M.; Muizebelt, W.J.; Klaasen, R.P.; Zabel, K.H. Mechanistic study of drying of alkyd resins using (Z,Z)- and (E,E)-3,6-nonadiene as model substances. *Prog. Org. Coat.* **1997**, *31*, 331–340. [[CrossRef](#)]
7. Erben, M.; Veselý, D.; Vinklárek, J.; Honzíček, J. Acyl-substituted ferrocenes as driers for solvent-borne alkyd paints. *J. Mol. Catal. A Chem.* **2012**, *353–354*, 13–21. [[CrossRef](#)]
8. Muizebelt, W.J.; Hubert, J.C.; Venderbosch, R.A.M. Mechanistic study of drying of alkyd resins using ethyl linoleate as a model substance. *Prog. Org. Coat.* **1994**, *24*, 263–279. [[CrossRef](#)]
9. De Boer, J.W.; Wesenhagen, P.V.; Wenker, E.C.M.; Maaijen, K.; Gol, F.; Gibbs, H.; Hage, R. The quest for cobalt-free alkyd paint driers. *Eur. J. Inorg. Chem.* **2013**, *21*, 3581–3591. [[CrossRef](#)]
10. Dubrulle, L.; Lebeuf, R.; Thomas, L.; Fressancourt-Collinet, M.; Nardello-Rataj, V. Catalytic activity of primary and secondary driers towards the oxidation and hydroperoxide decomposition steps for the chemical drying of alkyd resin. *Prog. Org. Coat.* **2017**, *104*, 141–151. [[CrossRef](#)]
11. Clennan, E.L.; Pace, A. Advances in singlet oxygen chemistry. *Tetrahedron* **2005**, *61*, 6665–6691. [[CrossRef](#)]
12. Erich, S.J.F.; Gezici-Koç, Ö.; Michel, M-E.B.; Thomas, C.A.A.M.; van der Ven, L.G.J.; Huinink, H.P.; Flapper, J.; Duivenvoorde, F.L.; Adan, O.C.G. The influence of calcium and zirconium based secondary driers on drying solvent borne alkyd coatings. *Polymer* **2017**, *121*, 262–273. [[CrossRef](#)]
13. Lison, D.; De Boeck, M.; Verougstraete, V.; Kirsch-Volders, M. Update on the genotoxicity and carcinogenicity of cobalt compounds. *Occup. Environ. Med.* **2001**, *58*, 619–625. [[CrossRef](#)] [[PubMed](#)]
14. Magaye, R.; Zhao, J.; Bowman, L.; Ding, M. Genotoxicity and carcinogenicity of cobalt-, nickel- and copper-based nanoparticles. *Exp. Ther. Med.* **2012**, *4*, 551–561. [[CrossRef](#)] [[PubMed](#)]
15. Sosa, A.D.; Echeverría, M.D. Surface alterations produced in grinding of austempered ductile iron. *Procedia. Mater. Sci.* **2015**, *8*, 155–161. [[CrossRef](#)]
16. Bouwman, E.; van Gorkum, R. A study of new manganese complexes as potential driers for alkyd paints. *J. Coat. Technol. Res.* **2007**, *4*, 491–503. [[CrossRef](#)]
17. Oyman, Z.O.; Minga, W.; van der Linde, R.; van Gorkum, R.; Bouwman, E. Effect of [Mn(acac)₃] and its combination with 2,2'-bipyridine on the autoxidation and oligomerisation of ethyl linoleate. *Polymer* **2005**, *46*, 1731–1738. [[CrossRef](#)]
18. Warzeska, S.T.; Zonneveld, M.; van Gorkum, R.; Muizebelt, W.J.; Bouwman, E.; Reedijk, J. The influence of bipyridine on the drying of alkyd paints: a model study. *Prog. Org. Coat.* **2002**, *44*, 243–248. [[CrossRef](#)]
19. Honzíček, J.; Vinklárek, J. Chemical curing of alkyd resin catalyzed by benzoylferrocene: Performance, kinetics, and thickness effects. *J. Appl. Polym. Sci.* **2018**, *135*, 46184. [[CrossRef](#)]
20. Micciché, F.; Oostveen, E.; van Haveren, J.; van der Linde, R. The combination of reducing agents/iron as environmentally friendlier alternatives for Co-based driers in the drying of alkyd paints. *Prog. Org. Coat.* **2005**, *53*, 99–105. [[CrossRef](#)]
21. Pirš, B.; Znoj, B.; Skale, S.; Zabret, J.; Godnjavec, J.; Venturini, P. Iron as an alternative drier for curing of high-solid alkyd coatings. *J. Coat. Technol. Res.* **2015**, *12*, 965–974. [[CrossRef](#)]
22. Křížan, M.; Vinklárek, J.; Erben, M.; Císařová, I.; Honzíček, J. Autoxidation of alkyd resins catalyzed by iron(II) bispidine complex: Drying performance and in-depth infrared study. *Prog. Org. Coat.* **2017**, *111*, 361–370. [[CrossRef](#)]
23. Ha, D.; Joo, H.; Ahn, G.; Kim, M. J.; Bing, S.J.; An, S.; Kim, H.; Kang, K.-G.; Lim, Y.-K.; Jee, Y. Jeju ground water containing vanadium induced immune activation on splenocytes of low dose γ -rays-irradiated mice. *Food Chem. Toxicol.* **2012**, *50*, 2097–2105. [[CrossRef](#)] [[PubMed](#)]
24. Srivastava, A. K. Anti-diabetic and toxic effects of vanadium compounds. *Mol. Cell. Biochem.* **2000**, *206*, 177–182. [[CrossRef](#)] [[PubMed](#)]
25. Preininger, O.; Vinklárek, J.; Honzíček, J.; Mikysek, T.; Erben, M. A promising drying activity of environmentally friendly oxovanadium(IV) complexes in air-drying paints. *Prog. Org. Coat.* **2015**, *88*, 191–198. [[CrossRef](#)]
26. Preininger, O.; Charamzová, I.; Vinklárek, J.; Císařová, I.; Honzíček, J. Oxovanadium(IV) complexes bearing substituted pentane-2,4-dionate ligands: Synthesis, structure and drying activity in solvent-borne alkyd paints. *Inorg. Chim. Acta* **2017**, *462*, 16–22. [[CrossRef](#)]
27. Preininger, O.; Honzíček, J.; Kalenda, P.; Vinklárek, J. Drying activity of oxovanadium(IV) 2-ethylhexanoate in solvent-borne alkyd paints. *J. Coat. Technol. Res.* **2016**, *13*, 479–487. [[CrossRef](#)]

28. Lee, S.; Floriani, C.; Chiesi-Villa, A.; Guastini, C. Oxovanadium(IV) and dioxomolybdenum(VI) complexes: Synthesis from the corresponding acetylacetonato complexes and X-ray structures. *J. Chem. Soc. Dalton Trans.* **1989**, 145–149. [[CrossRef](#)]
29. ASTM International. *ASTM D5895-03 Standard Test Methods for Evaluating Drying or Curing During Film Formation of Organic Coating Using Mechanical Recorders*; ASTM International: West Conshohocken, PA, USA, 2008.
30. International Organization for Standardization. *ISO 1522:2006 Paints and Varnishes—Pendulum Damping Test*; International Organization for Standardization: Geneva, Switzerland, 2007.
31. Niewahner, J.H.; Walters, A.K.; Wagner, A. Improved synthesis of Geodken’s macrocycle through the synthesis of the dichloride salt. *J. Chem. Educ.* **2007**, *84*, 477–479. [[CrossRef](#)]
32. Wu, X.; Huang, T.; Lekich, T.T.; Sommer, R.D.; Weare, W.W. Synthesis of unsupported $d^1 - d^x$ oxido-bridged heterobimetallic complexes containing V^{IV} : A new direction for metal-to-metal charge transfer. *Inorg. Chem.* **2015**, *54*, 5322–5328. [[CrossRef](#)] [[PubMed](#)]
33. Smith, T.S., II; LoBrutto, R.; Pecoraro, V.L. Paramagnetic spectroscopy of vanadyl complexes and its applications to biological systems. *Coord. Chem. Rev.* **2002**, *228*, 1–18. [[CrossRef](#)]
34. Schumann, H. Zur Redoxchemie und Struktur von Oxovanadium(IV,V)-Komplexen mit substituierten Dibenzotetraaza[14]annulen Liganden. *Z. Naturforsch* **1995**, *50b*, 1494–1504. (In German)



© 2018 by the authors. Licensee MDPI, Basel, Switzerland. This article is an open access article distributed under the terms and conditions of the Creative Commons Attribution (CC BY) license (<http://creativecommons.org/licenses/by/4.0/>).